

Analytical Modeling of Metamaterial Absorbers with Low Cross-Polarized Reflected Field under Oblique Incidence using Equivalent Medium Approximation

Said Choukri^{1, 2, *}, Hakim Takhedmit¹, Otman El Mrabet², and Laurent Cirio¹

Abstract—In this paper, we propose a new physical model to accurately estimate the absorption characteristics in Metamaterial Perfect Absorbers (MPAs). The proposed model, relying on the reflection and refraction theory of microwaves, explains the physical mechanism of absorption and how unit-cell constitutive parameters can contribute to control the absorption characteristics. By considering Floquet modes (TE and TM) as two incident cross-polarized waves, analytical expressions have been established to estimate the absorption at normal and oblique incidences from the extracted constitutive parameters of the unit-cell. Analytical predictions are in excellent agreement with numerical results, proving the validity of our model. Furthermore, it can give an idea behind the absorption characteristics of MPA unit-cells without passing through full-wave simulation which usually takes time. Compared to previous works reported in the literature, the proposed method is efficient and does not require time-consuming tests and processing steps. Finally, analytical findings in this work hold for the general shapes of MPA resonators.

1. INTRODUCTION

Research on Metamaterial Perfect Absorbers (MPAs) is quite recent and is similar to what is done with absorbing materials comprising analog circuits, in particular Frequency Selective Surfaces (FSSs) [1]. The improvement provided by this kind of material compared to absorbers comprising analog circuits, like Salisbury screen [2] and Jaumann absorbers [3], consists in the reduction in the thickness of the structure. On the other hand, as they consist of periodic structures, made of dielectric and metallic materials, they are tunable and easier to fabricate. As a result of this metallo-dielectric arrangement, MPAs behave like a perfectly homogeneous material from an electromagnetic point of view [4]. These unprecedented electromagnetic properties make MPA a serious candidate to be used for several applications over wide frequency range starting from microwaves to optics, notably: electromagnetic energy harvesting [5, 6], Radar Cross Section (RCS) reduction [7], sensing applications [8], mutual coupling reduction in antenna arrays [9], switching [10], etc. The mechanism of perfect absorption of MPA at certain frequencies is explained by the matching process between the unit-cell intrinsic impedance and the free-space impedance [11]. When this condition is satisfied within the frequency band of interest, the reflection coefficient goes to zero leading to a near unity absorption rate, so that almost all incident electromagnetic energy is captured by the unit-cell. This can be considered as an overview explanation, and this approach is valid just when the electromagnetic (EM) waves are normally incident on the plane of the unit-cell. To give some insights into the mechanism of absorbing EM waves by MPA and further modeling and analysing this kind of EM absorbers, several models have been reported in

Received 8 February 2023, Accepted 23 May 2023, Scheduled 2 June 2023

* Corresponding author: Said Choukri (said.choukri@univ-eiffel.fr).

¹ ESYCOM, CNRS UMR 9007, Université Gustave Eiffel, F-77454 Marne-la-Vallée, France. ² LaSiT Lab, The Faculty of Sciences, Abdelmalek Essaadi University, BP 2121, Tetouan, Morocco.

the literature during the last decade. For instance, Transmission Line (TL) model was proposed by Wen et al. [12] to demonstrate the absorption mechanism of an electric Split Ring Resonator (eSRR) cell at THz frequencies. Based on this model, the absorption coefficient was calculated by computing the S -parameters of the TL-based model, but this model was limited to study just the case of normal incidence considering only the transverse electromagnetic (TEM) waves illumination, since a planar transmission line can only support the quasi-TEM mode. Furthermore, Pang et al. [13] analyzed a wire-based resonator metamaterial absorber by using an equivalent circuit approach. Also, this model was investigated in a restricted way only in normally incident TEM-polarized plane wave. Besides, via the presented circuit approach a loss of generality is noticed. In [14], a straightforward analysis was extended to study the absorption in oblique incidence based on interference theory developed by Chen [15] to interpret the electric/magnetic responses of MPA and the phase change introduced by the thickness of the dielectric spacer between the resonator and the ground plane. This model [14] gives a good estimation of absorption peaks in oblique incidence, but it is still so far a direct solver, and it is strongly related to the software simulation. By the way, for each value of the elevation angle (θ), the ground plane of the MPA unit-cell should be firstly removed (decoupled model), then the simulated magnitudes and phases of the scattering parameters can be exploited to calculate the absorption, which is a hard and time consuming task.

In this work, we propose a direct solving model which can be used to estimate the absorption characteristics of MPA structures under normal and oblique incidence conditions. By considering the two Floquet modes (TE and TM) as two incident plane waves, which corresponds to two orthogonal polarizations, analytical expressions for the absorption coefficient as a function of the unit-cell constitutive parameters were derived from the optic law of reflection and refraction. Without loss of generality, the proposed model can be adopted whatever the geometry of the absorbing cell being analyzed.

2. GENERAL CASE OF OBLIQUE INCIDENCE AT THE INTERFACE AIR-MPA UNIT-CELL

In this section, a comprehensive and exact mathematical description for the behaviour of MPA unit-cell illuminated by an oblique incident EM plane wave is explained and formulated for both TE and TM modes. We emphasize that the normal incidence is a case of particular interest when the angle of incidence θ_i goes to zero, so that general description of oblique incidence is held and extended to normal incidence. For the sake of simplicity, the azimuthal angle φ takes two values with respect to the polarization of the incident wave: ($\varphi = 90^\circ$ for TE and $\varphi = 0^\circ$ for TM). Hence, the analytical equations developed in this work do not show the azimuthal angle φ . As shown in Fig. 1, an incident forward oblique plane wave, with respect to the angle of incidence θ_i , illuminates the metallic resonator etched on the front side of a dielectric substrate. Note that in this model, we consider only the total electric and magnetic fields given by the superposition of the individual quantities. The metallic resonator and reflective ground plane, on the back side, have the metal thickness t_m and conductivity σ . The substrate is a dielectric slab of height h , relative permittivity ε_r , relative permeability μ_r , and dielectric loss tangent $\tan \delta$.

Due to the effective medium theory (EMT) [16], the MPA unit-cell can be considered as a homogeneous medium that has the effective impedance η_{eff} . As this impedance, seen looking into the front side of the unit-cell, is different from the free-space intrinsic impedance η_0 , a part of the incident power will be reflected back while the remaining part will be transmitted into the dielectric slab. In Fig. 1, θ_r and θ_t are, respectively, the reflection and transmission angles. At normal incidence ($\theta_i = 0^\circ$) of EM waves on the surface of the metamaterial absorber cell, the co-polarized and cross-polarized reflection coefficients at the interface air-MPA can be expressed for both TE (y -polarized wave) and TM (x -polarized wave) modes as follows:

$$\gamma^{kk}(\omega) = \frac{E_r^k(\omega)}{E_i^k(\omega)} \quad (1)$$

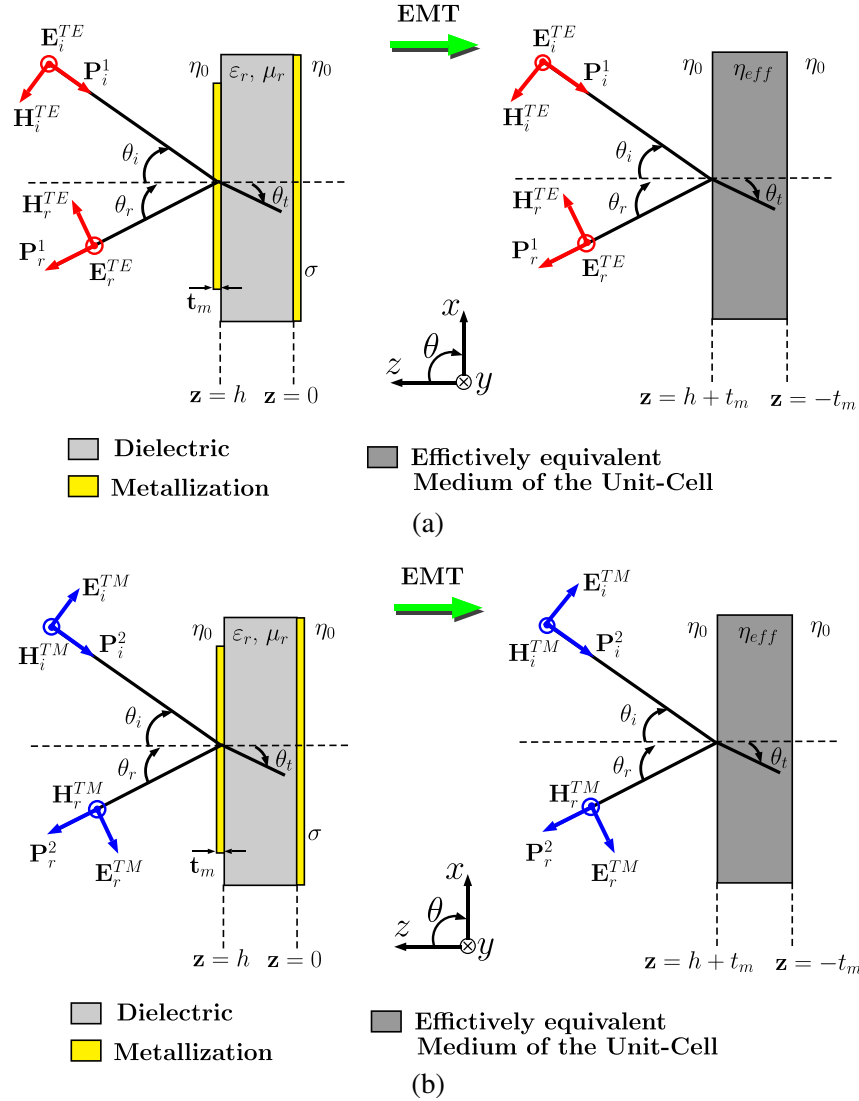


Figure 1. Reflection/Refraction of oblique incident plane wave at the front side of a MPA unit-cell and its equivalent effective medium representation based on EMT. (a) Case of TE. (b) Case of TM.

where $k = \{x, y\}$. For the cross-polarized reflection coefficient, we have:

$$\gamma^{kl}(\omega) = \frac{E_r^k(\omega)}{E_i^l(\omega)} \quad (2)$$

where $l = \{x, y\}$ for $k = \{y, x\}$.

By applying the superposition theorem to the reflected electric field components, the total reflection coefficient can be written as follows:

$$\gamma^k(\omega) = \gamma^{kk}(\omega) + \gamma^{kl}(\omega) \quad (3)$$

Similarly, for the total transmission coefficient:

$$\tau^k(\omega) = \tau^{kk}(\omega) + \tau^{kl}(\omega) \quad (4)$$

We emphasize that τ^k is the transmission coefficient through the MPA cell to the air. In this work, we deal with MPA unit-cells that present a low cross-polarization conversion, so the contribution of the

reflected cross-component of the electric field can be ignored in (3) and (4). Therefore, the reflectivity and transmittance would be expressed respectively, by:

$$R^k(\omega) = \left| \gamma^k(\omega) \right|^2 = \left| \frac{\eta_{eff}^k(\omega) - \eta_0}{\eta_{eff}^k(\omega) + \eta_0} \right|^2 \quad (5)$$

$$T^k(\omega) = \left| \tau^k(\omega) \right|^2 \quad (6)$$

where ω is the angular frequency. Due to the presence of full reflective metallic ground plane in MPA structures to block the transmission through, no transmission occurs over the whole frequency band ($\tau^k(\omega) \approx 0$). Besides, the absorption coefficient could be expressed only in terms of the reflectivity as follows:

$$A^k(\omega) = 1 - R^k(\omega) \quad (7)$$

The normalized effective impedance can also be expressed only in terms of the reflection characteristics of the unit-cell as follows:

$$\eta_{eff}^k(\omega) = \sqrt{\frac{\mu_{eff}^k(\omega)}{\varepsilon_{eff}^k(\omega)}} = \frac{1 + (\gamma^k(\omega))^2}{1 - (\gamma^k(\omega))^2} \quad (8)$$

It should be noted that reflection coefficients and effective impedances are complex quantities. The normalized constitutive parameters of the unit-cell can be extracted from simulated or measured frequency responses using Reflection Only (RO) algorithm [17]:

$$\varepsilon_{eff}^k(\omega) = 1 + \chi_e^k(\omega) = 1 + \frac{2j}{\beta_0(\omega)h} \left(\frac{1 - \gamma^k(\omega)}{1 + \gamma^k(\omega)} \right) \quad (9)$$

$$\mu_{eff}^k(\omega) = 1 + \chi_m^k(\omega) = 1 + \frac{2j}{\beta_0(\omega)h} \left(\frac{1 + \gamma^k(\omega)}{1 - \gamma^k(\omega)} \right) \quad (10)$$

In Equations (9) and (10), $\beta_0(\omega) = \omega\sqrt{\varepsilon_0\mu_0}$ is the propagation constant in free-space; χ_e^k and χ_m^k are, respectively, the complex electric and magnetic susceptibilities. From all above aforementioned relationships between the characteristics of MPA unit-cell and its reflection coefficient in the frequency domain, we can clearly notice the dependence of these characteristics on the polarization state of the electric field of the incident waves, and this polarization can then define how the shaped metallic resonator will behave towards the external excitation to create a strong electric and/or magnetic resonance. Since the main objective of this work is to give a direct estimation of the absorptivity in the case of oblique incident TE- and TM-polarized waves, we can use the constitutive parameters (ε_{eff}^k and μ_{eff}^k) as well as the effective impedance η_{eff}^k calculated at normally incident waves to formulate the reflectivity at oblique incidence.

When we consider the entire unit-cell equivalent to a homogeneous dielectric slab of effective impedance η_{eff} (Fig. 1), the reflection coefficient at the interface air-MPA unit-cell in TE and TM excitations at an incident angle θ_i is calculated by applying boundary conditions to the EM fields as follows:

$$\gamma^y(\omega, \theta_i) = \frac{E_r^y(\omega)}{E_i^y(\omega)} = \frac{\eta_{eff}^y(\omega) \cos \theta_i - \eta_0 \cos \theta_t}{\eta_{eff}^y(\omega) \cos \theta_i + \eta_0 \cos \theta_t} \quad (11)$$

$$\gamma^x(\omega, \theta_i) = \frac{E_r^x(\omega)}{E_i^x(\omega)} = \frac{\eta_{eff}^x(\omega) \cos \theta_t - \eta_0 \cos \theta_i}{\eta_{eff}^x(\omega) \cos \theta_t + \eta_0 \cos \theta_i} \quad (12)$$

Following notations of Fig. 1, Snell's law of reflection and refraction can be formulated by the following equations:

$$\theta_r = \theta_i \quad (13)$$

$$\beta_0 \sin \theta_i = \beta_{eff}^k(\omega) \sin \theta_t \quad (14)$$

where $\beta_{eff}^k(\omega)$ is the wavenumber in the effectively equivalent medium of the unit-cell, which can be expressed by:

$$\beta_{eff}^k(\omega) = \omega \sqrt{\varepsilon_0 \varepsilon_{eff}^k \mu_0 \mu_{eff}^k} = \beta_0 \sqrt{\varepsilon_{eff}^k \mu_{eff}^k} \quad (15)$$

Replacing $\beta_{eff}^k(\omega)$ by its expression in Eq. (14) we obtain:

$$\theta_t = \arcsin \left(\frac{\sin \theta_i}{\sqrt{\varepsilon_{eff}^k \mu_{eff}^k}} \right) = \arcsin(\psi(\theta_i)) \quad (16)$$

where:

$$\psi(\theta_i) = \frac{\sin \theta_i}{\sqrt{\varepsilon_{eff}^k \mu_{eff}^k}}$$

This new expression of Snell's law, given by (16), leads to eliminating θ_t from Equations (11) and (12), hence:

$$\gamma^y(\omega, \theta_i) = \frac{\eta_{eff}^y(\omega) \cos \theta_i - \eta_0 \cos(\arcsin(\psi(\theta_i)))}{\eta_{eff}^y(\omega) \cos \theta_i + \eta_0 \cos(\arcsin(\psi(\theta_i)))} \quad (17)$$

$$\gamma^x(\omega, \theta_i) = \frac{-\eta_0 \cos \theta_i + \eta_{eff}^x(\omega) \cos(\arcsin(\psi(\theta_i)))}{\eta_0 \cos \theta_i + \eta_{eff}^x(\omega) \cos(\arcsin(\psi(\theta_i)))} \quad (18)$$

This formulation, given by Equations (17) and (18), provides a simplified and direct method to calculate the reflection coefficient for TE and TM modes at any incident angle if the effective impedance and constitutive parameters of the unit-cell are known at normal incidence. However, the absorption coefficient is expressed for TE and TM modes by:

$$A^y(\omega, \theta_i) = 1 - R^y(\omega, \theta_i) = 1 - |\gamma^y(\omega, \theta_i)|^2 \quad (19)$$

$$A^x(\omega, \theta_i) = 1 - R^x(\omega, \theta_i) = 1 - |\gamma^x(\omega, \theta_i)|^2 \quad (20)$$

Figure 2 describes the flowchart used to estimate the absorption coefficients ($A^x(\omega, \theta_i)$ or $A^y(\omega, \theta_i)$) in oblique incidence from the unit-cell constitutive parameters extracted initially from only one EM simulation at normal incidence, unlike [14] where EM simulations were running in each step of the angle θ_i .

3. NUMERICAL SIMULATION AND MODEL VALIDATION

In order to evaluate the performances of this model, the MPA unit-cell proposed in our earlier work [18] has been served as a testing sample to prove the validity of our analytical findings. Fig. 3 illustrates the schematic of the metamaterial absorber unit-cell with its geometrical parameters, where the host material is an epoxy FR-4 lossy substrate, having a relative permittivity of $\varepsilon_r = 4.3 \times (1 - j0.025)$, and the metallic resonator is made of copper which has the conductivity $\sigma = 5.8 \times 10^7$ S/m. The geometrical parameters have been optimized to fix the resonance frequency at 5.8 GHz. It should be mentioned that the unit-cell presents a low cross-polarized reflection coefficient of -45 dB at the resonance frequency. Following the first step described in the flowchart (Fig. 2), the unit-cell has been analysed under normal incidence by using Floquet modal analysis utility in CST MWS software. Indeed, *unit-cell* boundary conditions have been applied in the x and y directions to simulate a 2D infinite periodic array, while two Floquet ports were used to excite the two Floquet modes TE and TM. Then, the simulated reflection coefficients have been used to accurately extract the unit-cell constitutive parameters, using the above described RO algorithm, as well as its effective impedance. As shown in Fig. 4, the normalized real part of the unit-cell effective impedance is equal to 1 ($\Re\{\eta_{eff}^k\} = \eta_0$), while the imaginary part is equal to zero at the resonance frequency (5.8 GHz) for both TE (Figure 4(a)) and TM (Figure 4(b)) excitations. It can also be seen from Fig. 4 that the frequency response of the unit-cell is similar for the two modes, and this effect can be readily explained by the high symmetry of the impinging wave and structure under

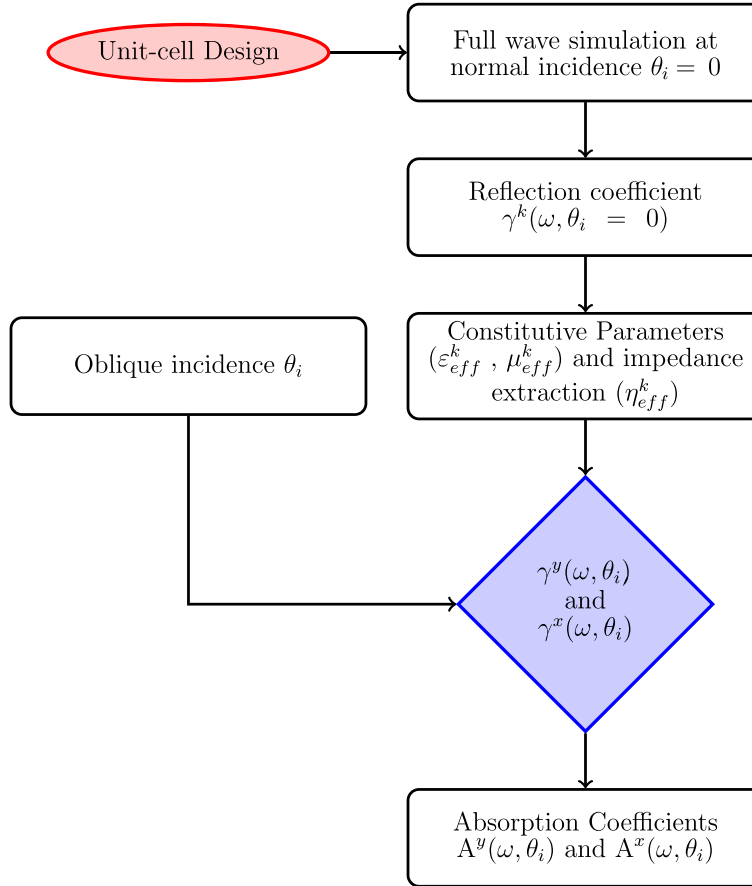


Figure 2. Step by step flowchart model for absorption estimation in oblique incidence from unit-cell response under normal incidence.

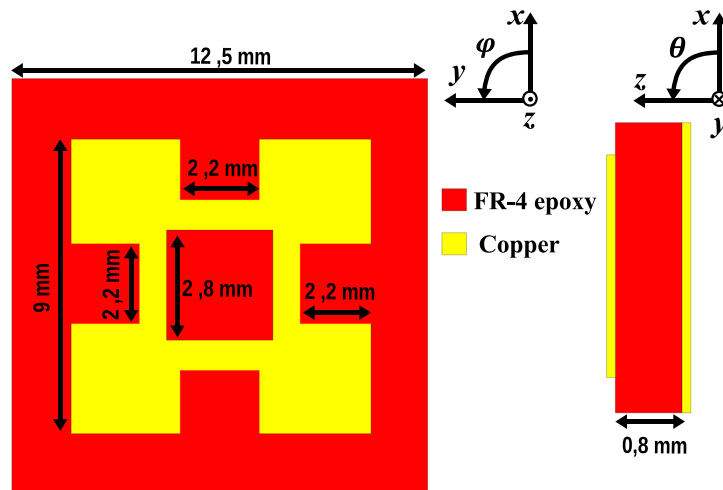


Figure 3. Schematic of absorbing unit-cell considered here to validate the proposed analytical model.

normal incidence. Based on the extracted effective impedances and by using Equations (17) and (18), the reflection coefficient has been calculated under various incident angles. Fig. 5 shows a very good agreement between EM simulations and analytical results, except that for the sake of symmetry when the incidence angle approaches 90° , a bit difference in terms of reflection magnitudes appears between

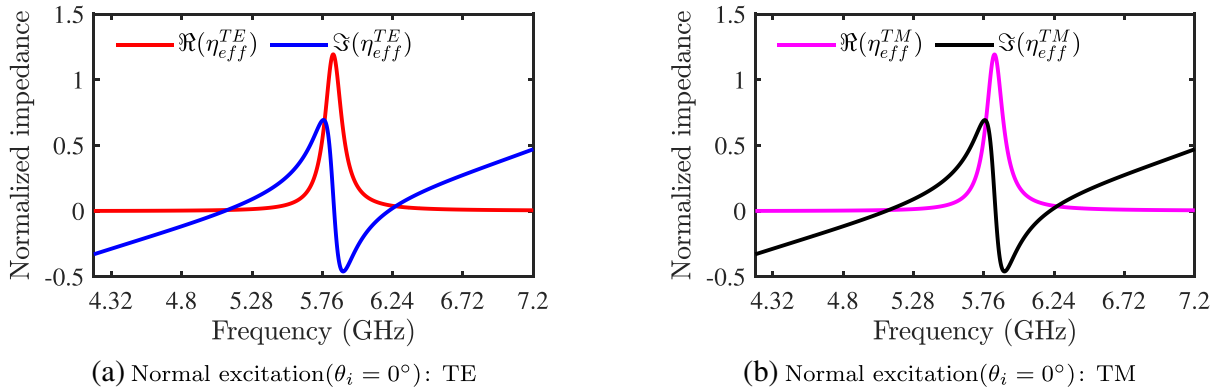


Figure 4. Normalized equivalent effective impedance of the unit-cell as a function of frequency: (a) Case of TE mode excitation, and (b) case of TM mode excitation.

analytical calculations and simulations, especially around the resonance frequency.

Finally, the absorptivity of the unit-cell has been calculated analytically with respect to different incident angles θ_i using expressions described by Equations (17), (18), (19), and (20). The comparison between numerically simulated results and analytically calculated ones is reported in Fig. 6. We have performed calculations with incident angle step width of 5 degrees, but we limited to show results with wider step of 20 degrees in Figs. 5 and 6. Besides, we can observe that there is an excellent agreement between analytical and simulated absorption curves over the whole frequency span for both TE and TM modes. We also note that the proposed model can accurately predict the decay of absorption rate as the angle of incidence increases, which is a real challenge in designing MPAs. However, achieving perfect absorption with incident angle insensitivity is a much complicated mission due to the impedance mismatching issues when approaching the critical angle. Although, as mentioned before, when approaching the grazing angle (The 90-degree complement to angle of incidence) an estimation error appeared between the simulation results and those calculated by the analytical model especially at the resonance frequency, due to the symmetry of impinging waves, leading to a small increase in the impedance mismatching, the oblique incident wave sees different effective impedances from the normal one. But the error of estimation is still lower, only 4% for TM mode, and even much lower than that for the TE mode.

In order to verify how the change in quality factor would impact the calculation results, we have plotted the simulated and calculated quality factors as a function of the incident angle θ_i . It is defined as:

$$Q = \frac{f_0}{FWHM} \quad (21)$$

where f_0 is the frequency point of the maximum absorption, and $FWHM$ is the Frequency Width at Half Maximum. As we have seen before (Fig. 6), there is a slight difference between the simulated and calculated absorption peaks for TM mode when the angle of incidence increases, and this aspect can be explained by the quality factor change. As shown in Fig. 7, for higher values of the quality factor (Fig. 7(a)) the analytically calculated absorption curves agree perfectly with simulated ones as can be seen in Fig. 6 for TE mode result. On the other hand, when the quality factor decreases (less than 19) a slight difference appears between the analytical and simulated results, as can be seen in Fig. 6 for TM mode absorption curves.

From the above results, we can claim that the proposed model is efficient and less consuming EM simulation tasks for absorption coefficients prediction than previous limited analyses in [12–14]. Further comparisons between the method developed in this work and others reported in the literature are presented in Table 1.

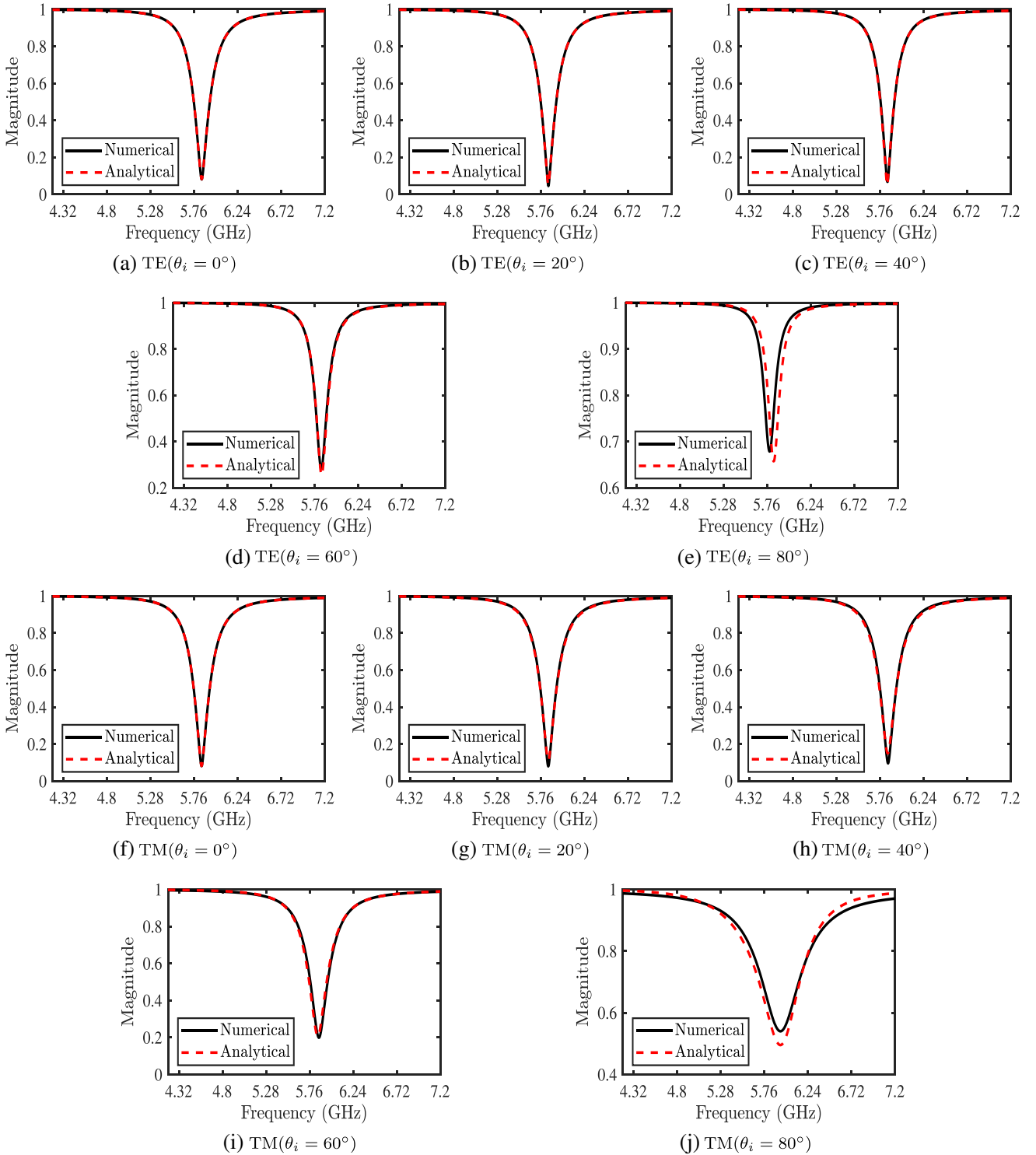


Figure 5. Comparison between numerically simulated and analytically calculated reflection coefficients for different values of the incidence angle θ_i : (a), (b), (c), (d) and (e) Case of TE. (f), (g), (h), (i) and (j) Case of TM.

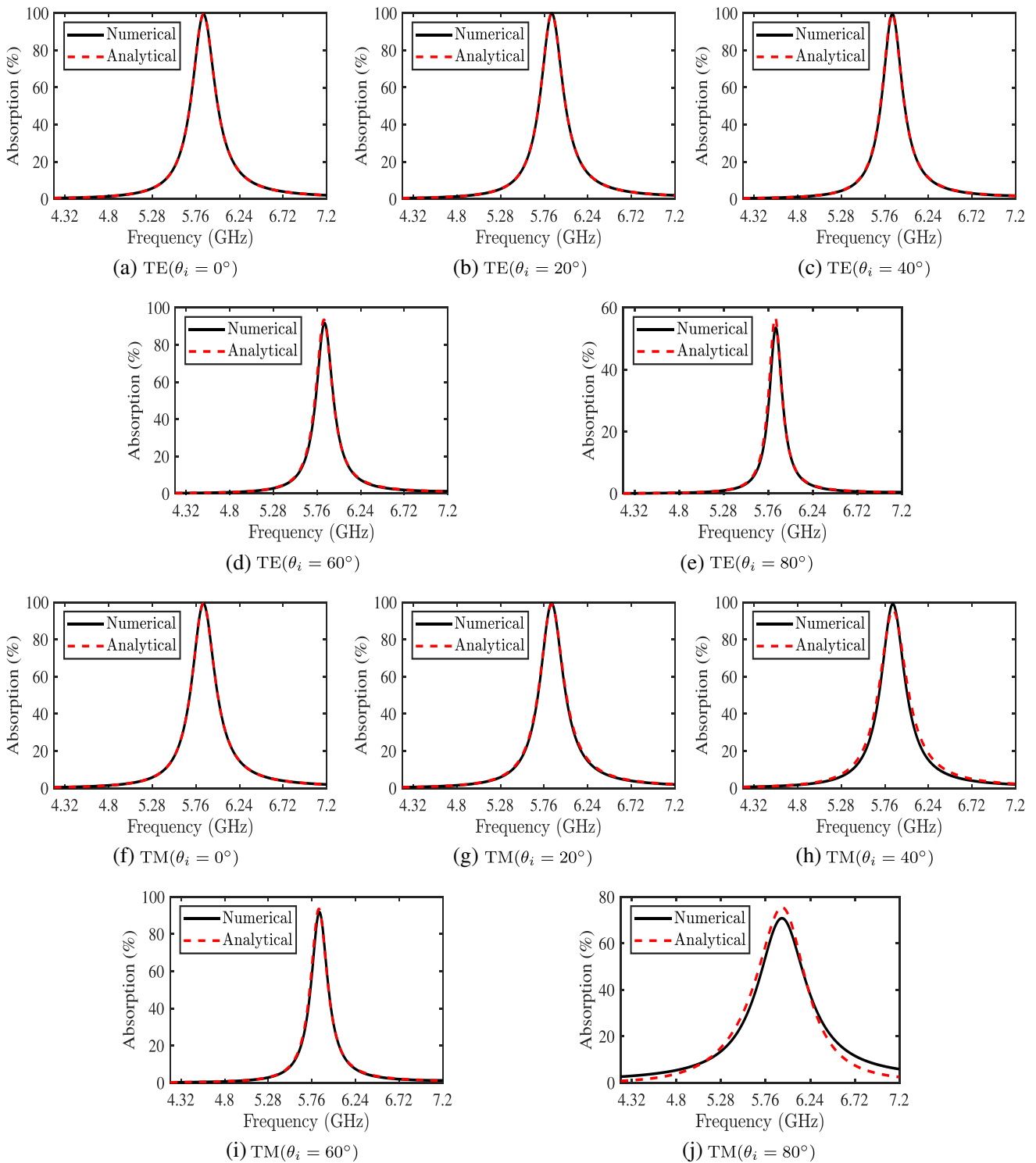


Figure 6. Comparison between numerically simulated and analytically calculated absorption curves for different values of the incidence angle θ_i . (a), (b), (c), (d) and (e) Case of TE. (f), (g), (h), (i) and (j) Case of TM.

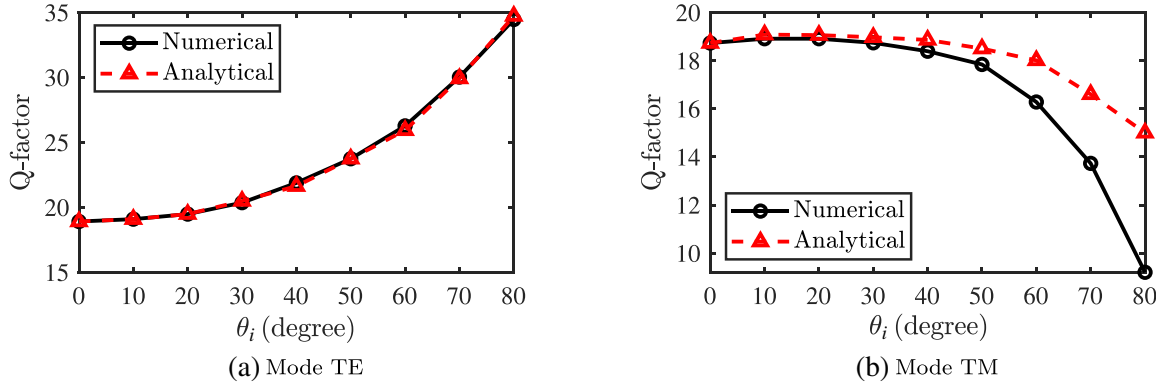


Figure 7. Corresponding change of the quality factor of the unit-cell as a function of the incidence angle θ_i : (a) Case of TE-polarized wave excitation and (b) TM-polarized wave excitation.

Table 1. Summary of the comparison between the proposed work and the earlier reported ones in the literature.

Ref.	Model based theory	Incident Wave Analyse	Polarizations	EM simulation Tasks
Ref. [12]	Transmission Line	Normal	TEM	One ^a
Ref. [13]	Equivalent Circuit Approach	Normal	TEM	One ^a
Ref. [14]	Interference Theory	Normal and Oblique	TE and TM	Two for each incident angle ^b
This work	Equivalent Medium Theory	Normal and Oblique	TE and TM	One^a

^aOne EM simulation is performed to extract the S -parameters at normal incidence ($\theta_i = 0^\circ$).

^bTwo EM simulations are performed to extract the S -parameters at each value of the incidence angle (θ_i): One simulation with ground plane (coupled model) and the second without ground plane (decoupled model).

4. CONCLUSION

In summary, we developed a novel and efficient model based on classical theory of reflection and refraction and the effective medium theory. The proposed model not only can be used to estimate analytically the absorption coefficients, but also gives some insights on how these coefficients are directly related to the unit-cell effective impedance and its constitutive parameters compared to the existing models proposed in the literature. Beside these merits, the proposed model drastically decreases the computational time compared to the model based on the interference. Our model has been tested at microwave frequencies leading to a better result, which is in a good agreement with full wave simulation.

ACKNOWLEDGMENT

This work was carried out within the framework of Toubkal Project TBK/20/100 Campus No. 43761TJ. The authors thank Campus France and the partenariats Hubert Curien Program (PHC).

REFERENCES

1. Mishra, R., R. Panwar, and D. Singh, "Equivalent circuit model for the design of frequency-selective, terahertz-band, graphene-based metamaterial absorbers," *IEEE Magnetics Letters*, Vol. 9, 1–5, 2018, Art no. 3707205, doi: 10.1109/LMAG.2018.2878946.
2. Zhou, Z., K. Chen, B. Zhu, J. Zhao, Y. Feng, and Y. Li, "Ultra-wideband microwave absorption by design and optimization of metasurface salisbury screen," *IEEE Access*, Vol. 6, 26843–26853, 2018, doi: 10.1109/ACCESS.2018.2835815.
3. Liang, M. and D. Hao-Chuan, "The absorbing characteristics of plasma-filled double-layer Jaumann screen," *2021 International Applied Computational Electromagnetics Society (ACES-China) Symposium*, 1–2, 2021, doi: 10.23919/ACES-China52398.2021.9581551.
4. Hakim, M. L., T. Alam, Md. S. Islam, et al., "Wide-oblique-incident-angle stable polarization-insensitive ultra-wideband metamaterial perfect absorber for visible optical wavelength applications," *Materials*, Vol. 15, 1996–1944, 2022, doi: 10.3390/ma15062201.
5. Dinh, M., N. Ha-Van, N. T. Tung, and M. Thuy Le, "Dual-polarized wide-angle energy harvester for self-powered IoT devices," *IEEE Access*, Vol. 9, 103376–103384, 2021, doi: 10.1109/ACCESS.2021.3098983.
6. Ashoor, A. Z., T. S. Almoneef, and O. M. Ramahi, "A planar dipole array surface for electromagnetic energy harvesting and wireless power transfer," *IEEE Transactions on Microwave Theory and Techniques*, Vol. 66, No. 3, 1553–1560, Mar. 2018, doi: 10.1109/TMTT.2017.2750163.
7. Zhang, Z., Y. Zhang, T. Wu, et al., "Broadband RCS reduction by a quaternionic metasurface," *Materials MDPI*, Vol. 14, 2787, 2021.
8. Mohanty, A., O. P. Acharya, B. Appasani, S. K. Mohapatra, and M. S. Khan, "Design of a novel terahertz metamaterial absorber for sensing applications," *IEEE Sensors Journal*, Vol. 21, No. 20, 22688–22694, Oct. 15, 2021, doi: 10.1109/JSEN.2021.3109158.
9. Garg, P. and P. Jain, "Isolation improvement of MIMO antenna using a novel flower shaped metamaterial absorber at 5.5 GHz WiMAX band," *IEEE Transactions on Circuits and Systems II: Express Briefs*, Vol. 67, No. 4, 675–679, Apr. 2020, doi: 10.1109/TCSII.2019.2925148.
10. Chen, K., X. Zhang, S. Li, et al., "Switchable 3D printed microwave metamaterial absorbers by mechanical rotation control," *J. of Physics D: Applied Physics*, Vol. 53, No. 30, 305105, May 2020.
11. Tao, H., N. I. Landy, C. M. Bingham, X. Zhang, R. D. Averitt, and W. J. Padilla, "A metamaterial absorber for the terahertz regime: Design, fabrication and characterization," *Opt. Express*, Vol. 16, 7181–7188, 2008.
12. Wen, Q.-Y., Y.-S. Xie, H.-W. Zhang, Q.-H. Yang, Y.-X. Li, and Y.-L. Liu, "Transmission line model and fields analysis of metamaterial absorber in the terahertz band," *Opt. Express*, Vol. 17, 20256–20265, 2009.
13. Pang, Y., H. Cheng, Y. Zhou, and J. Wang, "Analysis and design of wire-based metamaterial absorbers using equivalent circuit approach," *Journal of Applied Physics*, Vol. 113, 114902, 2013.
14. Wanghuang, T., W. Chen, Y. Huang, and G. Wen, "Analysis of metamaterial absorber in normal and oblique incidence by using interference theory," *AIP Advances*, Vol. 3, 102118, 2013, <https://doi.org/10.1063/1.4826522>.
15. Chen, H.-T., "Interference theory of metamaterial perfect absorbers," *Opt. Express*, Vol. 20, 7165–7172, 2012.
16. Shaltout, A., V. Shalaev, and A. Kildishev, "Homogenization of bi-anisotropic metasurfaces," *Opt. Express*, Vol. 21, 21941–21950, 2013.
17. De Araujo, J. B. O., G. L. Siqueira, E. Kemptner, M. Weber, C. Junqueira, and M. M. Mosso, "An ultrathin and ultrawideband metamaterial absorber and an equivalent-circuit parameter retrieval method," *IEEE Transactions on Antennas and Propagation*, Vol. 68, No. 5, 3739–3746, May 2020, doi: 10.1109/TAP.2020.2963900.
18. Choukri, S., H. Takhedmit, O. El Mrabet, and L. Cirio, "Energy harvesting using loaded metamaterial absorber unit-cell with polarization independent capability," *10th National Days on Energy Harvesting and Storage (JNRSE)*, Grenoble, France, 2021.